Open Access

Open Journal of Internet of Things (OJIOT)
Volume 2, Issue 1, 2016
http://www.ronpub.com/ojiot
ISSN 2364-7108

A 24 GHz FM-CW Radar System for Detecting Closed Multiple Targets and Its Applications in Actual Scenes

Kazuhiro Yamaguchi [A], Mitumasa Saito [B], Takuya Akiyama [A], Tomohiro Kobayashi [A], Naoki Ginoza [A], Hideaki Matsue [A]

[A] Tokyo University of Science, Suwa, 5000-1 Toyohira, Chino, Nagano, Japan, 391-0292, yamaguchi@rs.tus.ac.jp, GH14601@ed.tus.ac.jp, GH15607@ed.tus.ac.jp, G112033@ed.tus.ac.jp, matsue@rs.suwa.tus.ac.jp

[B] CQ-S net Inc., Torigoe 7-8, Kanagawa-ku, Yokohama-shi, Kanagawa, Japan, 221-0064, saitoh@kpe.biglobe.ne.jp

Abstract

This paper develops a 24 GHz band FM-CW radar system to detect closed multiple targets in a small displacement environment, and its performance is analyzed by computer simulation. The FM-CW radar system uses a differential detection method for removing any signals from background objects and uses a tunable FIR filtering in signal processing for detecting multiple targets. The differential detection method enables the correct detection of both the distance and small displacement at the same time for each target at the FM-CW radar according to the received signals. The basic performance of the FM-CW radar system is analyzed by computer simulation, and the distance and small displacement of a single target are measured in field experiments. The computer simulations are carried out for evaluating the proposed detection method with tunable FIR filtering for the FM-CW radar and for analyzing the performance according to the parameters in a closed multiple targets environment. The results of simulation show that our 24 GHz band FM-CW radar with the proposed detection method can effectively detect both the distance and the small displacement for each target in multiple moving targets environments. Moreover, we develop an IoT-based application for monitoring several targets at the same time in actual scenes.

Type of Paper and Keywords

Regular research paper: *24 GHz, FM-CW radar, distance measuring, small displacement measuring, multiple targets detection, tunable FIR filtering*

1 Introduction

Recently, rapidly evolving wireless communication technologies enable us to obtain various piece of information from a lot of manufacturers in the wide range of the technology field. The IoT (Internet of things) is a key topic in network field for developing systems and services, and it enables various physical devices to collect various pieces of information such as sensor information. Radar has been used as a sensing application to detect in wide range of areas such as on the ground, on the sea, in the air, and in space. Radar systems can detect various pieces of information according to the application area by transmitting and receiving using radio waves.

Twenty-four GHz band radar systems are based on

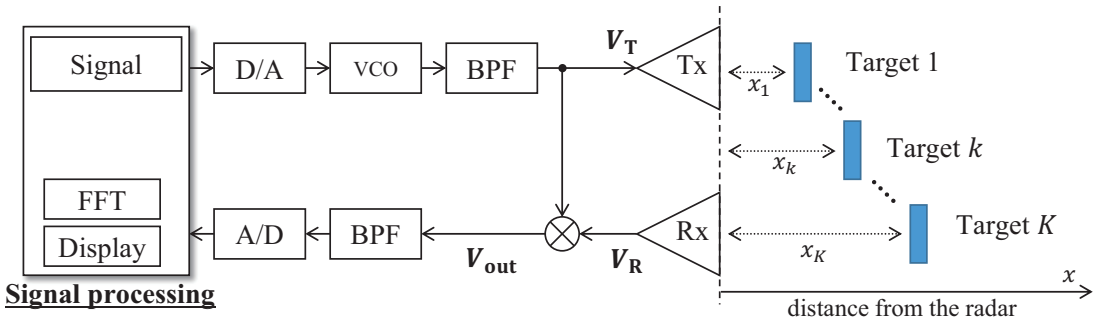

Figure 1: Block diagram of FM-CW radar system

the ARIB standard T73 [2] in Japan as sensors for detecting or measuring mobile objects for a specified low power radio station. And the 24 GHz band radar system can be applied to various fields such as security and medical imaging in indoor and outdoor environments. Various radar systems have been reported [11, 16, 6, 19]. Pulsed radar systems can measure the period between the transmitted and received signals. Pulsed radars can detect the distance in the far field. However, the targets in the near field cannot be detected correctly by a pulsed radar. Doppler radar systems can measure the frequency difference between the transmitted and reflected signals. A Doppler radar can detect the moving velocity of the target, but it cannot detect the distance of the target. FM-CW (Frequency-Modulated Continuous-Wave) radar systems [12, 3, 13, 17, 1] are the most widely used for detecting the distance of the target object in the near field and the small displacement of the target. In MIMO (Multiple-Input Multiple-Output) radar systems [9, 5], several radars are used at the same time for measuring the target's information. In these radar systems, each radar has both advantages and disadvantages. Therefore, the types of radars are determined according to the necessary information and the situation.

In this paper, we focused on an FM-CW radar system to detect human breathing in the near field. In a previous study, we reported the design, performance analysis, and applications when using a 24 GHz band radar system to detect both the distance from the radar and the small displacement caused by human breathing [21]. The radar system could correctly detect both the distance to the human from the radar and the small displacement caused by the human breathing. However, it was difficultto detect the distances and displacements for multiple humans at the same time. To detect the distances and displacements in a closed multiple target environment, we proposed a detection method for signal processing with a tunable FIR (Finite Impulse Response) filter [4] in the FM-CW radar system [20]. Furthermore, a performance analysis for the FM-CW radar system was performed using computer simulations.

In this paper, the proposed detection method considers both the differential detection and the tunable FIR filtering to detect both the distances and small displacements in single and closed multiple target environments. The results of the computer simulations show that the proposed FM-CW radar system with FIR filtering could detect targets correctly when the distance between targets was greater than 0.5 m. Moreover, applications based on the IoT for detecting human movements in actual scenes were described by using the developed FM-CW radar system. The IoT-based radar system could collect information on the breathing of several people by using network transmission. The results show that the FM-CW radar system could detect human breathing in actual scenes, and the IoT-based radar system would monitor the human breathing remotely.

The rest of this paper is organized as follows. In Section 2, we describe the principle of the FM-CW radar system and its basic performance in a single target environment. Section 3 presents the proposed detection method in a single target environment, and Section 4 presents the proposed detection method in a multiple target environment. In Section 5, we discuss the results of the computer simulation and field experiments. Finally, Section 6 concludes this paper.

2 FM-CW Radar System

In this section, a basic system model of the FM-CW radar and basic performance for measuring a distance and a small displacement of a target in a computer simulation are described.

2.1 Principle of FM-CW Radar

Figure 1 shows the block diagram of an FM-CW radar system [15]. FM-CW radar is a type of radar that

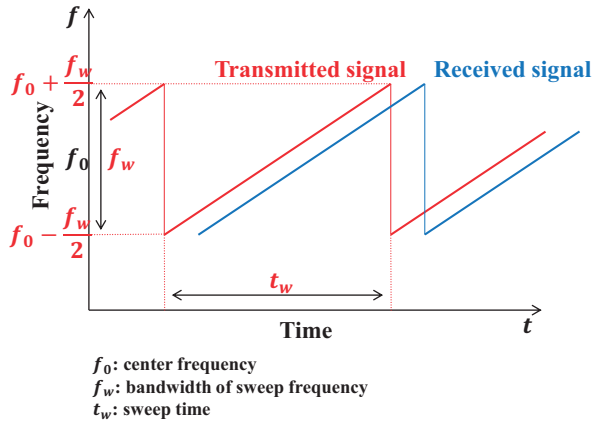

Figure 2: Sawtooth frequency modulation

transmits a continuous carrier modulated by a periodic function, such as a sawtooth wave, to provide the range data. In Figure 1, VCO means voltage-controlled oscillator, D/A means digital-to-analog conversation, BPF means bandpass filter, and A/D means analog-to-digital conversation.

In the FM-CW radar system, the frequency modulated signal at the VCO is transmitted from transmitter Tx; then, signals reflected from the targets are received at receiver Rx. The transmitted and received signals are multiplied by a mixer, and beat signals are generated by multiplying the two signals. The beat signals pass through a low pass filter, and an output signal is then obtained. In this process, the frequency of the input signal is varied with time at the VCO. The modulation waveform has a linear sawtooth pattern [14] (shown in Figure 2). This figure illustrates the frequency-time relation in the FM-CW radar; the red line denotes the transmitted signal, and the blue line denotes the received signal which has some delay time. Here, f_0 denotes the center frequency, f_{w} denotes the bandwidth of sweep frequency, and t_w denotes the sweep time.

The transmitting signal $V_{\mathrm{T}}(f,x)$ is represented as

$$V_{\mathrm{T}}(f,x) = A\mathrm{e}^{j\frac{2\pi f}{c}x} \quad , \tag{1}$$

where f denotes the frequency at a certain time, x denotes the distance from the transmitter whose position is $x = 0$, A denotes the amplitude value of the transmitted signal, and c denotes the speed of light.

The reflected signal $V_{\mathrm{R}}(f,x)$ is represented as

$$V_{\mathrm{R}}(f,x) = \sum_{k=1}^{K} A\alpha_k\gamma_k\mathrm{e}^{j\varphi_k}\mathrm{e}^{j\frac{2\pi f}{c}(2d_k-x)} \quad , \tag{2}$$

where γ_k and φ_k are the reflective coefficients for the amplitude and phase of the kth target, respectively. α_k denotes the amplitude coefficient for transmission loss from the kth target, and d_k is the distance between the transmitter and the kth target.

Here, at the receiver whose position is $x = 0$, Equation (2) is rewritten as

$$V_{\mathrm{R}}(f,0) = \sum_{k=1}^{K} A\alpha_k\gamma_k\mathrm{e}^{j\varphi_k}\mathrm{e}^{j\frac{2\pi f}{c}(2d_k)} \quad . \tag{3}$$

The beat signal is generated by multiplying the transmitted signal in Equation (1) by the received signal in Equation (3) at the position $x = 0$. After passing through an LPF, the output signal $V_{\mathrm{out}}(f,0)$ is generated by

$$V_{\mathrm{out}}(f,0) = \sum_{k=1}^{K} A^2\alpha_k\gamma_k\mathrm{e}^{j\varphi_k}\mathrm{e}^{j\frac{4\pi f d_k}{c}} \quad . \tag{4}$$

By using signal processing, the distance and displacement for the target are given from the generated output signal in Equation (4). By using Fourier transform, the distance spectrum of the output signal $P(x)$ is calculated as follows.

$$\begin{aligned} P(x) &= \int_{f_0-\frac{f_w}{2}}^{f_0+\frac{f_w}{2}} V_{\mathrm{out}}\mathrm{e}^{-j\frac{4\pi f}{c}}df \\ &= \int_{f_0-\frac{f_w}{2}}^{f_0+\frac{f_w}{2}} \sum_{k=1}^{K} A^2\alpha_k\gamma_k\mathrm{e}^{j\varphi_k}\mathrm{e}^{j\frac{4\pi f d_k}{c}}\mathrm{e}^{-j\frac{4\pi f x}{c}}df \\ &= A^2\sum_{k=1}^{K}\alpha_k\gamma_k\mathrm{e}^{j\varphi_k}\int_{f_0-\frac{f_w}{2}}^{f_0+\frac{f_w}{2}}\mathrm{e}^{j\frac{4\pi f(d_k-x)}{c}}df \\ &= A^2\sum_{k=1}^{K}\left[\alpha_k\gamma_k\mathrm{e}^{j\varphi_k}\mathrm{e}^{j\frac{4\pi f_0(d_k-x)}{c}}\right. \\ &\qquad \left.\cdot f_w\mathrm{sinc}\left\{\frac{2\pi f_w(d_k-x)}{c}\right\}\right] \quad . \end{aligned} \tag{5}$$

In this equation, the function of $\mathrm{sinc}(x)$ denotes

$$\mathrm{sinc}(x) = \frac{\sin x}{x} \quad . \tag{6}$$

The amplitude value of the distance spectrum $|P(x)|$ in

Equation (5) is given as

$$|P(x)| = A^2 \left| \sum_{k=1}^{K} \alpha_k \gamma_k \mathrm{e}^{j\varphi_k} \mathrm{e}^{j\frac{4\pi f_0 (d_k - x)}{c}} \cdot f_w \mathrm{sinc}\left\{ \frac{2\pi f_w (d_k - x)}{c} \right\} \right|$$
$$\leq A^2 f_w \sum_{k=1}^{K} \left[\alpha_k \gamma_k \cdot \left| \mathrm{sinc}\left\{ \frac{2\pi f_w (d_k - x)}{c} \right\} \right| \right] , \quad (7)$$

and we have equality if and only if the phase components $\phi_k + \frac{4\pi f_0 (d_k - x)}{c}$ for all of k are equal.

Here, we assumed that the number of targets is 1. The distance spectrum in Equation (5) is rewritten as

$$P(x) = \left[A^2 \alpha_1 \gamma_1 \mathrm{e}^{j\varphi_1} \mathrm{e}^{j\frac{4\pi f_0 (d_1 - x)}{c}} \cdot f_w \mathrm{sinc}\left\{ \frac{2\pi f_w (d_1 - x)}{c} \right\} \right] , \quad (8)$$

and the amplitude value of the distance spectrum is given as

$$|P(x)| = A^2 \alpha_1 \gamma_1 f_w \left| \mathrm{sinc}\left\{ \frac{2\pi f_w (d_1 - x)}{c} \right\} \right| . \quad (9)$$

This equation indicates that the distance of the target is generated by the amplitude value of the distance spectrum.

The phase value of the distance spectrum $\angle P(x)$ is represented as

$$\angle P(x) = \varphi_1 + \frac{4\pi f_0 (d_1 - x)}{c} = \theta_1(x) . \quad (10)$$

Here, because $\theta_1(x)$ satisfies $-\pi \leq \theta_1(x) \leq \pi$, the displacement of the target is

$$-\frac{c(-\pi - \varphi_1)}{4\pi f_0} \leq d_1 \leq \frac{c(\pi - \varphi_1)}{4\pi f_0} . \quad (11)$$

If the phase value satisfies $\phi_1 = 0$, Equation (11) is rewritten as -3.11 [mm] $\leq d_1 \leq +3.11$ [mm] with $f_0 = 24.15$ [GHz]. That is, a small displacement of the target within ± 3.11 [mm] is generated by the phase value of the distance spectrum.

On the other hand, the maximum distance for measuring $d_{\max}$ is

$$\Delta f = \frac{f_w}{t_w / t_s} [\mathrm{Hz}] ,$$
$$d_{\max} = \frac{c}{4\Delta f} [\mathrm{m}] , \quad (12)$$

Table 1: Parameters in computer simulations

Parameters	Values
Center frequency f_0	24.15 (GHz)
Bandwidth of sweep frequency f_w	50, 100, 200, 400 (MHz)
Sweep time t_w	1024 (μs)
Sampling time for sweep	0.1, 1, 10 (μs)
Number of FFT points	4096
Window function	hamming

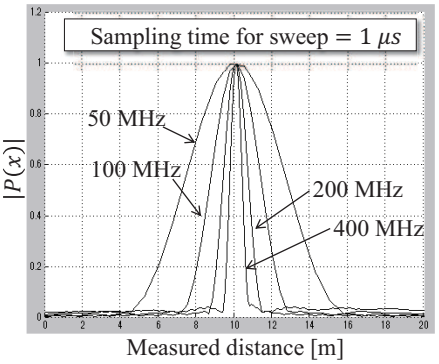

Figure 3: Range resolution for distance spectrum according to bandwidth of sweep frequency f_w

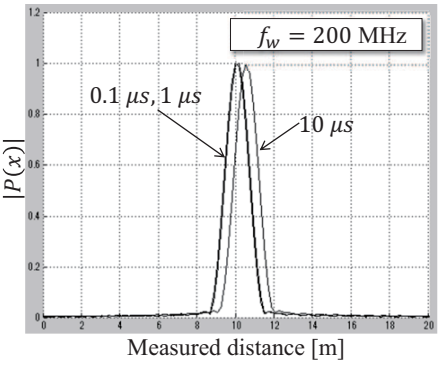

Figure 4: Error value for distance spectrum according to sampling time for sweep

where t_w denotes the sweep time, t_s denotes the interval time for sampling, and Δf denotes the frequency resolution of the distance spectrum. For example, in the case when t_w = 1024 μs and t_s = 1 μs, the maximum distance $d_{\max}$ is 384 [m].

2.2 Analysis of Basic Performance

First, we describe the basic performance of the 24 GHz band FM-CW radar. The parameters for the computer simulation are listed in Table 1 and were determined in accordance with ARIB standard T73 [2]. The center

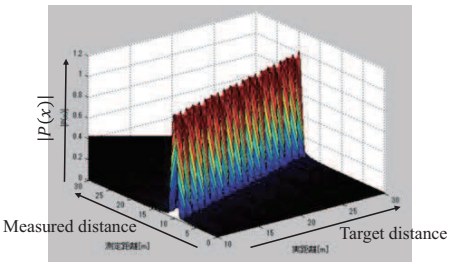

(a) 3D view.

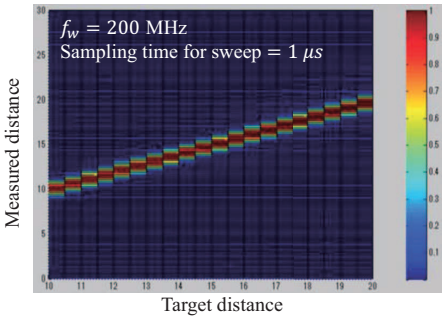

(b) 2D view.

Figure 5: Distance spectrum for measuring moving target

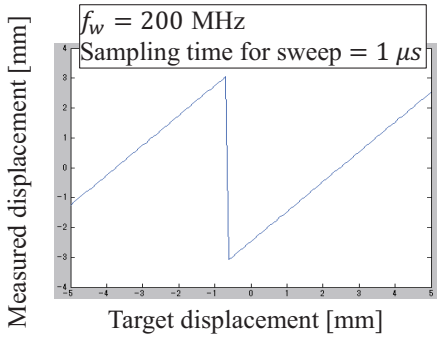

Figure 6: Measured displacement

frequency was 24.15 GHz, and the bandwidths were 50, 100, 200, and 400 MHz. Note that the 400 MHz bandwidth was only used for the computer simulation because of radio law standards in Japan. The sweep time was 1024 μs, sampling times for the sweep were 0.1, 1, and 10 μs, number of FFT points was 4096, and the hamming windows were used as the window function in signal processing.

We assumed that a static target was located at 10 meters from the transmitter and receiver, and the distance spectrums were outputted with various parameters. Figure 3 shows the amplitude value for the distance spectrum versus the measured distance with various sweep bandwidths. The results show that the sweep bandwidth affected the range resolutions of the measured distance, and a widely swept bandwidth could improve the range resolution. In the case when t_s = 1 μs, the range resolutions of the measured distance with f_{w} = 50, 100, 200, and 400 MHz were $\pm$5, $\pm$1.5, $\pm$1, and $\pm$0.5 m, respectively. Figure 4 shows the amplitude value for the distance spectrum versus the measured distance with various sampling time. The results show that the sampling interval affected the error of the measured distance, and a short sampling interval could reduce the error value for the distance. In the case when f_w = 200 MHz, the error value of the measured distance with t_s = 10 μs was about 0.5 m.

Figure 5 shows the results for measuring a slowly moving target when f_w = 200 MHz and t_s = 1 μs. The target moved slowly from a distance of 10 m to 20 m with intervals of 0.5 m. Figure 5(a) shows the amplitude value versus the measured distance versus the target distance (shown in 3-dimensional view), Figure 5(b) shows the measured distance versus the target distance (shown in 2-dimensional view). The color in (b) corresponds to the strength of the amplitude value in (a). From these figures, it was confirmed that the distance could be measured correctly according to the positions of the moving target.

Figure 6 shows the results of measuring a target with small displacement, and the measured displacement versus the target displacement was outputted. The object was located at 10m from the receiver, and the object moved from -5mm to 5mm with intervals of 0.1mm. A small displacement could be measured by the phase value of the distance spectrum, and the measured displacement corresponds to the target displacement. Note that the measured displacement denotes the relative displacement, and it does not correspond to the absolute distance between the receiver and the target object. A small displacement was correctly measured within $\pm$ 3.11 mm with the parameters of the FM-CW radar system in this paper although a displacement of more than $\pm$3.11 mm let to uncertainty.

3 Proposed Techniques for Single Target Detection

To detect a target's information accurately, such as distance and small displacement, we propose an algorithm for eliminating the signals reflected from the background objects. This section describes the proposed algorithm and shows the results of computer simulations and field experiments.

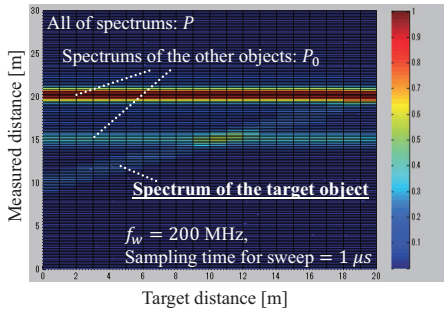

(a) Without differential detection

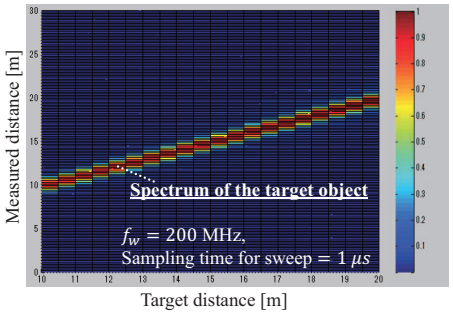

(b) With differential detection (Proposed)

Figure 7: Distance spectrum for measuring moving target distance with / without differential detection in environments in which multiple objects are located.

3.1 Detection for Single Targets

As mentioned in the above section, the FM-CW radar system could measure the distance and the small displacement at the same time for a single target. However, being able to receive only the reflected signal on the target at the receiver was a special case. Generally, the receiver receives signals reflected from many objects including the desired target. Therefore, when there were several objects, signal processing for detecting the distance spectrum from only the desired target was required.

The proposed method removed the signals from the other objects by using the differential detection of distance spectrum. Figure 7 shows the distance spectrum when the target object moved from a distance of 10m to 20m, and the other objects were located at a distance of 15m and 20m. The transmitted signal was reflected on the target and the other objects, and the receiver received several reflected signals. Therefore, the distance spectrum of the other objects was also generated by the FM-CW radar system in Figure 7(a), and the distance spectrum of the target could not be detected accurately. In particular, when the reflection coefficient of the target was lower than that of the other objects, the distance spectrum of the other objects had a higher amplitude value than that of the target.

In the proposed differential detection, the distance spectrum of the other objects P_0 was first generated beforehand (shown in Figure 7(a)). The distance spectrum P_0 was generated when there were no people for detecting the distance and the small displacement. Then, the distance spectrum of both the target and the other targets P, which includes P_0, was subtracted by P_0. By using the differential detection, the distance spectrum of the target and the other targets was removed from the distance spectrum of the other targets P_0. Therefore, only the distance spectrum of the desired target $P - P_0$ was detected. Figure 7(b) shows the distance spectrum by using the proposed differential detection method, and the distance spectrum of the target was correctly measured. Compared with the measured distance spectrums in Figure 7(a) and (b), it was clearly confirmed that the proposed method could detect the target distance by using the differential detection. The proposed differential detection could effectively detect the distance of a moving or static target from multiple reflections of the background static objects.

Table 2: Parameters in field experiments

Parameters	Values
Center frequency f_0	24.15 (GHz)
Bandwidth of sweep frequency f_w	200 (MHz)
Sweep time t_w	1024 (μs)
Sampling time for sweep t_s	1 (μs)
Output power on transmission	7 (mW)
Antenna gain	11 (dBi)
Range of distance	0–100 (m)
Range of relative displacement	$\pm$3.11 (mm)

3.2 Field Experiments and Applications

In this section, we describe setup conditions and results of field experiments, and demonstrates the IoT-based FM-CW radar application.

3.2.1 Setup Conditions for Field Experiments

To evaluate the effectiveness of the proposed method for detecting the target distance and displacement, we developed a FM-CW radar system and carried out the experiments with the radar system in an actual environment. Table 2 lists the parameters. The developed FM-CW radar system obtained a certificate of conformity with regard to the technical regulations

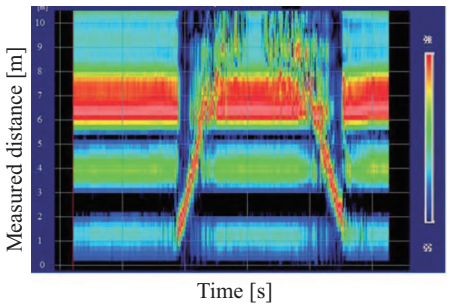

(a) Without differential detection

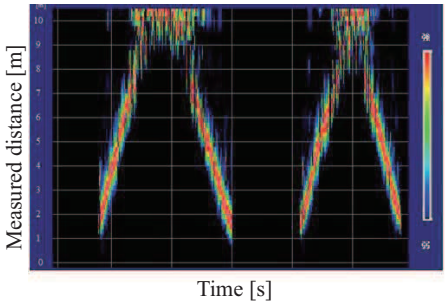

(b) With differential detection (Proposed)

Figure 8: Distance spectrum for measuring moving target distance with / without differential detection.

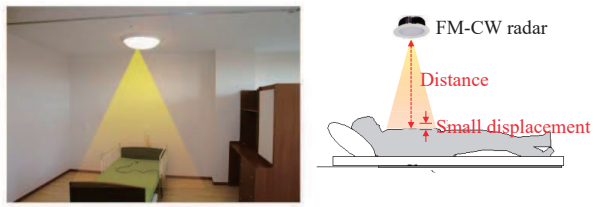

Figure 9: Setting example of FM-CW Radar for detecting human breathing

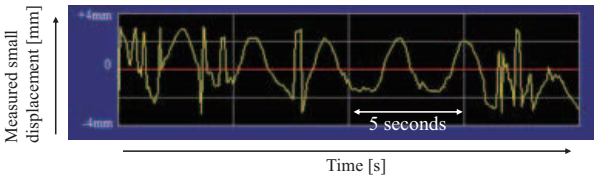

Figure 10: Displacement for measuring movement of human breathing

in Article 38-6, paragraph 1 of the radio law [18] in Japan, and the developed FM-CW radar system satisfied the ARIB standard T73 in Japan [2].

3.2.2 Results of Field Experiments

Figure 8 shows the distance spectrum of a moving target. A person walked away from the FM-CW radar and then came close between 2m to 10m. In Figure 8(a), several distance spectrums of the person and the background objects were outputted. The distance spectrum of the moving person was not clearly detected in Figure 8(a) because of the signals reflected from background objects. To detect the distance spectrum of the moving person by the differential detection method, the distance spectrum without the person was measured beforehand. By generating the distance spectrum of the background objects beforehand, the distance spectrum of the moving person was correctly detected in Figure 8(b) with the proposed differential detection. Therefore, the FM-CW radar system could measure the movement of the target person effectively.

Figure 9 shows the setup of the FM-CW radar system for detecting human breathing in actual scenes. The FM-CW radar satisfied the safety guidelines, and the details of the safety guidelines are described in the Appendix. Figure 10 shows the results of measuring the small displacement for human breathing. The person's chest movement was measured within the range of relatively small displacement. In Figure 10, the period of breathing was detected to be about 4s, and the breathing movement was detected within $\pm$2mm.

3.2.3 Examples of Applications

In this section, we show an example of application of the 24 GHz band FM-CW radar system in a hospital. Figure 11(a) shows an example of the results for detecting the human breathing of a single target in a room in the hospital. The distance spectrum in this example was measured as follows.

1. Measuring the distance spectrum without any people.
2. A person comes to the bed. The radar receives signals from the person's body.
3. The person lies asleep on the bed. The radar detects the person's breathing movement.

By generating the distance spectrum of the background objects without the person, only the distance spectrum of the person was detected. When the person comes within the range of the radar, the radar system could detect the signals reflected from the person, and the distance spectrums of the person's body were detected. Once the person had laid down on the bed, the radar system could detect the small displacement due to the person's breathing. By using the differential detection method,

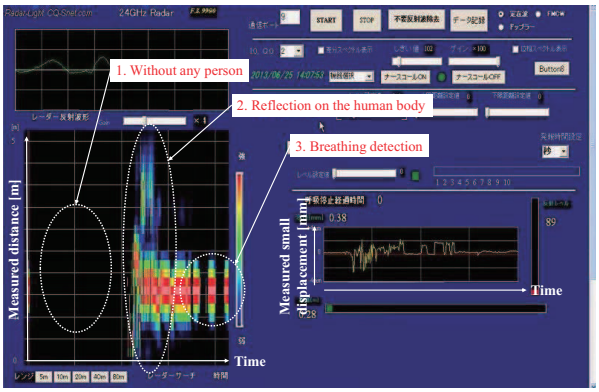

(a)

(b)

Figure 11: Examples of applications of the FM-CW radar system

the distance and small displacement of the moving object were accurately detected.

By connecting the developed FM-CW radars in several rooms in the hospital, detecting several targets could be achieved through accessing the network. An example of monitoring several targets is shown in Figure 11(b). The developed FM-CW radars were connected to the network system, and the detected distance and small displacement data were sent to a server in the nurse station. In the nurse station, the status of several targets were collected and monitored, and alert information indicating, for example, falling out of bed and stopping breathing could be monitored. Although the trial experiments were just getting started, the remote monitoring of human breathing could help in hospital scenes.

4 Proposed Techniques for Multiple Target Detection

In this section, we improved the FM-CW radar system to detect multiple targets by using signal processing.

4.1 Multiple Target Detection Problems

As mentioned in the above section, the FM-CW radar system could detect both the distance and displacement

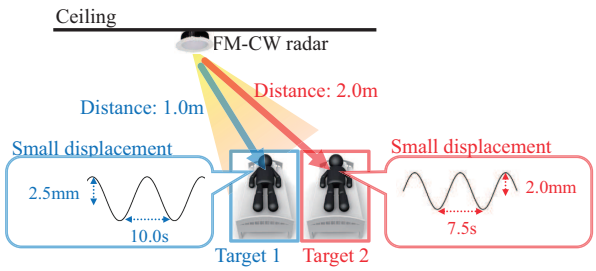

Figure 12: Setup with two targets

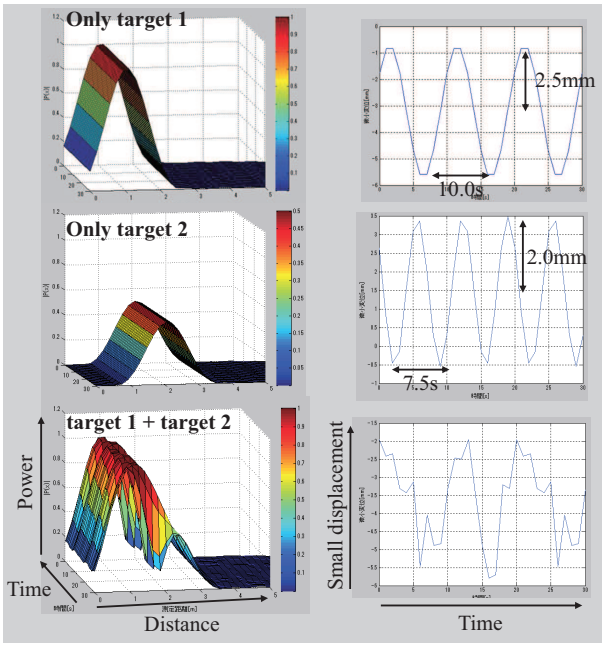

Figure 13: Simulated results of detection for closed multiple targets

correctly in single target environments. However, the FM-CW radar could not detect both the distance and displacement correctly in closed multiple targets environments. To detect closed multiple targets, we propose a detection method that uses the signal processing with a tunable FIR filter [4].

4.2 FIR Filtering

The procedures of the proposed detection method for multiple closed targets are as follows. We assumed that the FM-CW radar was located at a short distance from the beds as shown in Figure 12. Radio waves were emitted from the FM-CW radar, and the two targets laid down on their beds. The distances from the radar to each target were different, so the peaks of the distance spectrum were detected at different frequencies. In this case, the detected result shown on the bottom left in

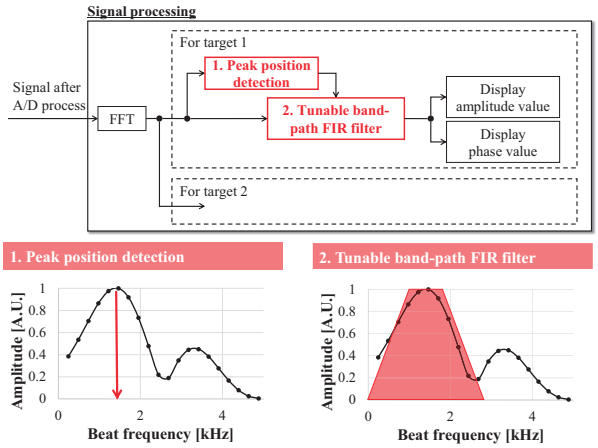

Figure 14: Block diagram of proposed multiple target detection in signal processing

Figure 13 was the sum of these two targets, and it was difficult to detect both the distance and phase values for each user correctly.

To solve this problem, signal processing with the tunable FIR filter was used in the proposed detection method. Figure 14 shows the block diagram of the proposed detection method. First, FFT was carried out on the A/D converted signal to obtain the distance spectrum. After FFT, the peaks of the amplitude value of the distance spectrum were calculated for each user. In the peak position detection processing, the two frequency values relating to the targets were obtained; then, FIR filters were designed according to the peak positions of the desired targets. The tunable FIR filter had a center frequency corresponding to the calculated frequency in the peak position detection, and had the linear property for the phase value. By using the designed FIR filter, bandpass filtering was carried out for the distance spectrum. After passing through the bandpass filter, the amplitude and phase value for each target were detected correctly.

4.3 Computer Simulations

To ebaluate the effectiveness of the proposed FIR filtering method, computer simulations were carried out. This section describes the setup conditions and the results of the computer simulations.

4.3.1 Setup Conditions

The parameters for the computer simulations are listed in Table 3 and are based on the ARIB standard T73 [2]. The center frequency was 24.15 GHz, and the frequency bandwidths were 100, 200, 400, and 800 MHz. Note that the 400 and 800 MHz bandwidths were only used for the computer simulation because of the radio law standards in Japan. The sweep times were 256, 512, 1024, and 2048 μs, sampling time of the sweep was 0.1 μs, number of FFT points was 4096, and the hamming windows were used as the window function in signal processing. The bandwidths for FIR filter were 200, 400, 800, 1600, and 3200 Hz. Table 4 lists positions, amplitudes, and phases of target 1 and target 2.

Table 3: Parameters in computer simulations

Parameters	Values
Center frequency f_0	24.15 (GHz)
Bandwidth of sweep frequency f_w	100, 200, 400, 800 (MHz)
Sweep time t_w	256, 512, 1024, 2048 (μs)
Bandwidth for FIR filter B	200, 400, 800, 1600, 3200 (Hz)
Number of FFT points	4096
Window function	hamming

Table 4: Setup for targets

Parameters	Target 1	Target 2
Distance	1.0 (m)	2.0 (m)
Amplitude of Displacement	2.5 (mm)	2.0 (mm)
Period of displacement	10.0 (s)	7.5 (s)

In the following sections, we describe the evaluation values for analyzing the results of multiple target detection, and the performance analysis according to the bandwidth for the sweep frequency, sweep time, bandwidth for FIR filter and position of target 2 were described.

4.3.2 Evaluation Values for Amplitude and Phase Values

Figure 15 shows the evaluation values for detecting the amplitude and phase values of the distance spectrum of multiple targets. As evaluation values, we defined the degree of amplitude separation for the amplitude value and NMSE (Normalized Mean Square Error) for the phase value.

The degree of amplitude separation is represented by

$$S_k = 10\log\frac{|P_{min}|}{|P_k|} = 10\log\frac{|P(f_{min})|}{|P(f_k)|}\ [\mathrm{dB}]\ , \quad (13)$$

where k denotes the number of targets, S_k denotes the degree of amplitude separation, P_{min} denotes the minimal value of the amplitude whose frequency is f_{min}, and P_k denotes the peak value for the k-th target with a frequency of f_k.

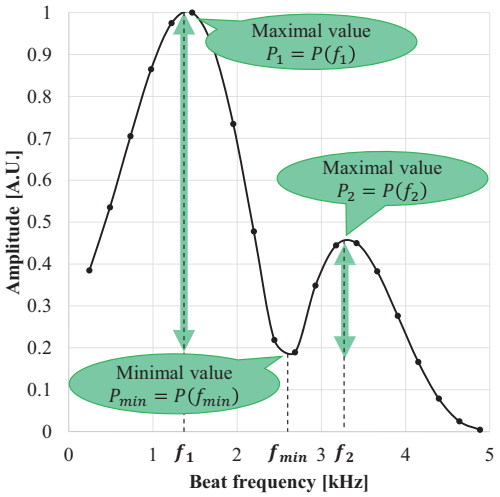

(a) Amplitude

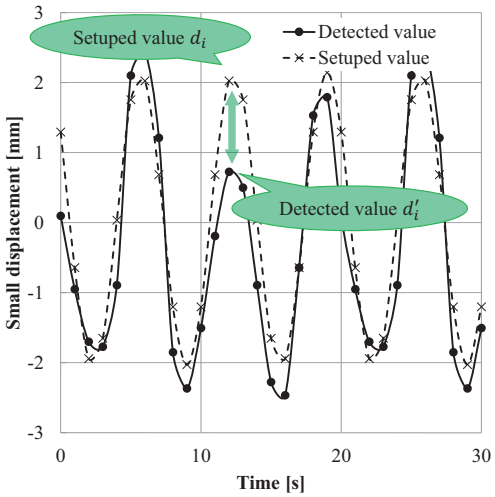

(b) Phase

Figure 15: Definitions of evaluation values for computer simulation

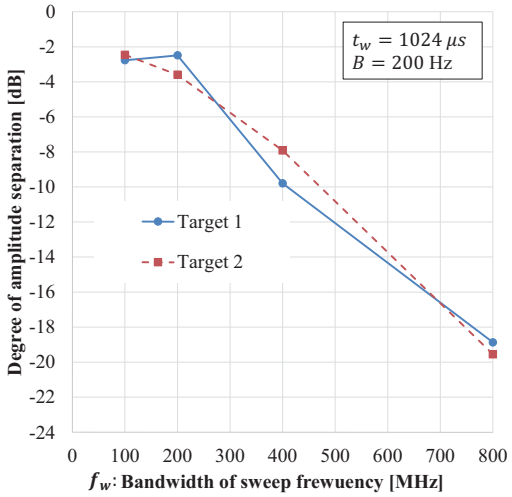

(a) Amplitude

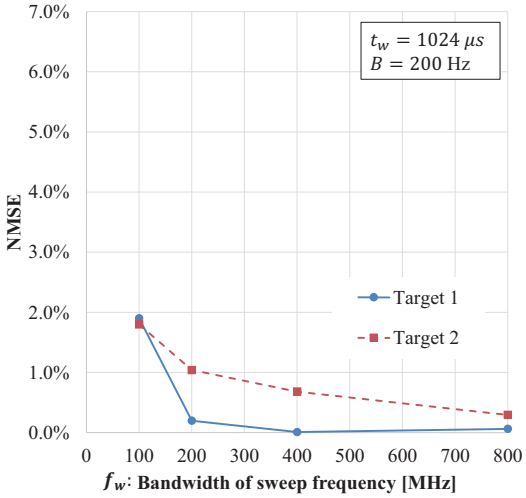

(b) Phase

Figure 16: Evaluation values versus bandwidth of sweep frequency

The NMSE for the phase value is represented by

$$\text{NMSE} = \sum_{i=1}^{N} \frac{|d_i' - d_i|^2}{|d_i'|^2} \quad , \tag{14}$$

where N denotes the number of sampling points, and d_i and d_i' denote the sampled signals of the detected and setup values for a target, respectively.

4.3.3 Performance for Bandwidth of Sweep Frequency

Figure 16 shows the evaluation values versus the bandwidth of sweep frequency f_w for (a) the amplitude value and (b) the phase value. As shown in (a), the degrees of amplitude separation were about -2.5 dB and -19 dB when $f_w = 100$ MHz and $f_w = 800$ MHz, respectively. Because the frequency resolution of the distance spectrum increased when increasing bandwidth of sweep frequency, separating the targets to determine the amplitude became easy.

As shown in (b), the NMSE was about 2 % when the bandwidth of sweep frequency $f_w = 100$ MHz, and the NMSE also improved when increasing bandwidth of sweep frequency. Although there were a few disadvantages relating to the NMSE of target 2, the multiple target detections could correctly be achieved because a degree of amplitude separation of -1 dB and an

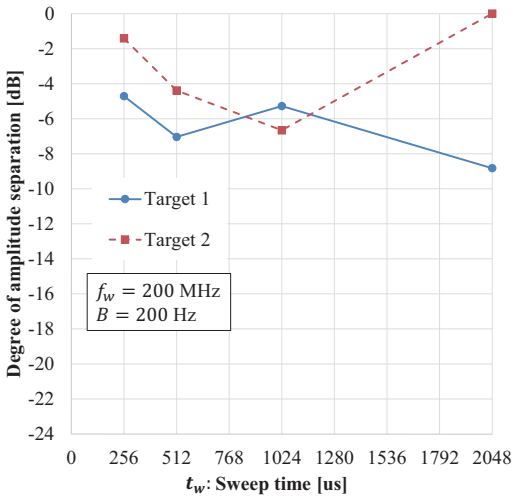

(a) Amplitude

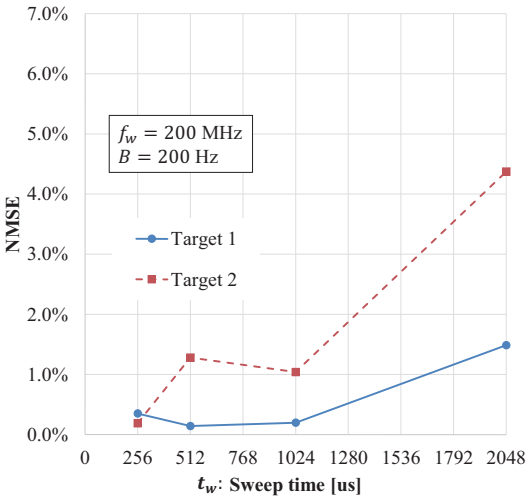

(b) Phase

Figure 17: Evaluation values versus sweep time

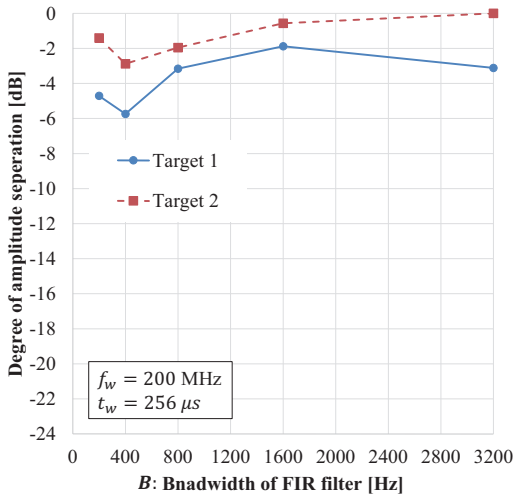

(a) Amplitude

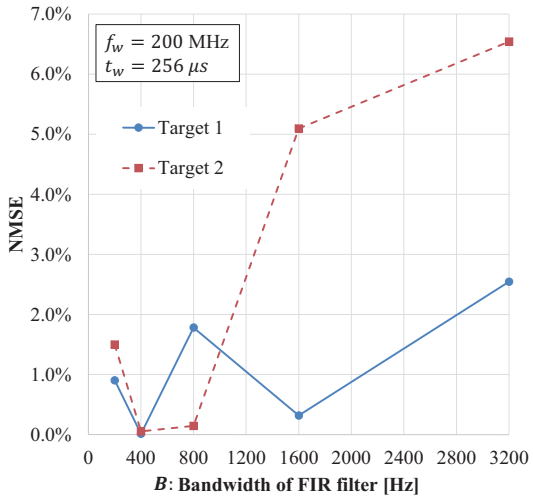

(b) Phase

Figure 18: Evaluation values versus bandwidth of FIR filter

NMSE of 6 % were high enough for detecting multiple targets in practical use.

4.3.4 Performance for Sweep Time

Figure 17 shows the evaluation values versus the sweep time t_w for (a) the amplitude value and (b) the phase value. As shown in (a), the degree of amplitude separation for target 1 kept at about -4 dB, which was not in accordance with the sweep time. The degree of separation for target 2 was -1 dB while the sweep time $t_w = 256 \sim 1024\ \mu s$. In the case when $t_w = 2014 \mu s$, the degree of amplitude separation was almost zero dB. That is, it was difficult to detect the peak value of the amplitude for target 2. Moreover, compared to the results in (b), the worst NMSE for target 2 was about 4 % when $t_w = 2048\ \mu s$. Because the resolution of the distance spectrum decreased with increasing sweep time, the sweep time should be less than 1024 μs.

4.3.5 Performance for Bandwidth of FIR Filter

Figure 18 shows the evaluation values versus the bandwidth of FIR filter B for (a) the amplitude value and (b) the phase value. As shown in (a), the degree of amplitude separation for target 1 kept at -2 dB, which was not in accordance with the bandwidth of FIR filter B. When bandwidth of FIR filter B was more than 1600 Hz, the degree was more than -1 dB. Therefore, it was

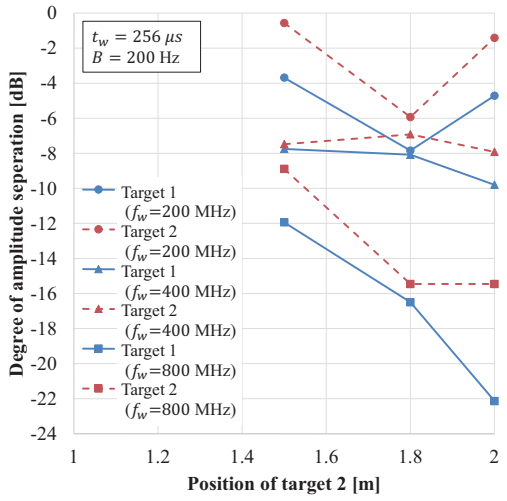

(a) Amplitude

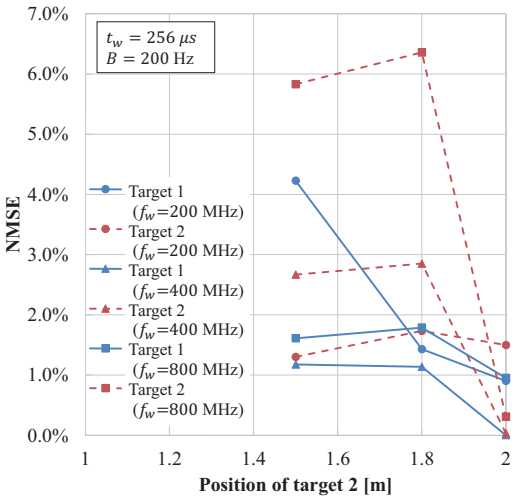

(b) Phase

Figure 19: Evaluation values versus positions of target 2

difficult to detect the peak value.

As shown in (b), the NMSE for target 1 was less than 3 %, but the NMSE for target 2 was more than 5 % when $B = 1600$ and 3200 Hz respectively. Because the wide bandwidth of the FIR filter was enough not to cut off the signal of the other target completely, the bandwidth of the FIR filter should be less than 1600 Hz.

4.3.6 Performance for Distance Between Targets

Finally, we show the results for detecting multiple targets when target 2 comes close to target 1 from a distance of 2 m to 1.5 m. Figure 19 shows the evaluation values versus the position of target 2 from the radar for (a) the amplitude value and (b) the phase value. The position of target 1 was 1 m from the radar.

Compared to the results, the degree of amplitude separation and NMSE became decreased as target 2 approaches target 1. As shown in (a), when the bandwidth of sweep frequency was more than 400 MHz, the degree of amplitude separation had good properties, which was enough to detect the peaks. However, in the case when $f_w = 200$ MHz, the degree for target 2 was about -0.3 dB, and it was difficult to detect the peaks.

As shown in (b), when f_w was less than 400 MHz, the NMSE could be kept at less than 5 %. However, in the case when $f_w = 800$ MHz, the NMSE decreased. It was difficult to detect the peaks of amplitude for targets as the distance between targets decreased. Therefore, the center frequency of the FIR filter was not enough to cut off the other target's signal, and the imperfect FIR filter affected the NMSE values. Although there were a few difficulties in determining the parameters of the proposed detecting method for FM-CW radar, the proposed detecting method could be effective for detecting the distance and the small displacement at the same time in multiple target environments.

5 Discussion

As for related work, MIT group reported a radar system for detecting human breathing [1]. The system could also detect movement, and the person breathing in the room could be detected accurately. However, in Japan, the bandwidth for sweep frequency was much smaller than that of the MIT's radar system because of the ARIB standard T73 [2]. As shown in Figure 3, the resolution of the distance spectrum depended on the bandwidth. Therefore, the smaller bandwidth affected the detected distance and small displacement. Moreover, in a closed multiple target environment, some distance between the radars and each target is required for distinguishing the distance spectrum of each target. Therefore, in this paper, we used a tunable FIR filtering method in signal processing to detect closed multiple targets at the same time.

In this paper, the computer simulated analysis was only described for detecting multiple targets at the same time. In the simulation, the huge computational cost of designing an FIR filter according to the position of the targets is required. Furthermore, in the field experiments, the proposed multiple target detection algorithm must be implemented on the hardware. As future work, we plan to analyze the performance taking into account the computational cost versus the filtering results to develop the FM-CW radar system with FIR filtering.

Moreover, for practical use of the IoT-based radar system, we have to analysis the performance of both the radar and network transmission. The number of the developed IoT-based radars is low, so the network performance requirements, such as throughput and end-to-end delay time, should be analyzed as future work.

6 Conclusion

In this paper, we developed a 24 GHz band FM-CW radar system for detecting the distance and small displacement of a target. The basic performance of a FM-CW radar was evaluated by using computer simulation, and the distance and small displacement of a single target were measured in field experiments. To detect both the distance and small displacement of multiple targets, we proposed a FM-CW radar system with a tunable FIR filter. The proposed detecting method generates a tunable FIR filter whose center frequency corresponds to the peak positions of the distance spectrum of each target. The tunable FIR filtered signal can be used to detect the distance and displacement for each target correctly. In computer simulations, the performance of the FM-CW radar system in a closed multiple moving target environment was analyzed in accordance with the bandwidth of sweep frequency, sweep time, bandwidth of FIR filter, and distance between targets. As a result, the 24 GHz band FM-CW radar with the proposed detection method could effectively detect both the distance and the small displacement for each target in multiple moving targets environments. And it was confirmed that the proposed detection method can detect both the distance and small displacement correctly when the distance between targets was greater than 0.5 m. Moreover, we developed an IoT-based application for monitoring several targets at the same time in actual scenes.

As future work, we will try to implement hardware for the proposed FIR filtering and carry out the field experiments.

Acknowledgements

Part of this work was supported by the "Ashita wo Ninau Kanagawa Venture Project" of Kanagawa, Japan. The authors thank Prof. Toshio Nojima at Hokkaido University in Japan for his valuable advice and for analyzing the safety aspects of the developed FM-CW radar system according to the safety guidelines.

References

[1] F. Adib, H. Mao, Z. Kabelac, D. Katabi, and R. C. Miller, "Smart homes that monitor breathing and heart rate," in *Proceedings of the 33rd Annual ACM Conference on Human Factors in Computing Systems*, ser. CHI '15. New York, NY, USA: ACM, April 2015, pp. 837–846.

[2] *ARIB STD-T73 Rev. 1.2, Sensors for Detecting or Measuring Mobile Objects for Specified Low Power Radio Station*, http://www.arib.or.jp/english/html/overview/doc/1-STD-T73v1_2.pdf, Association of Radio Industries and Businesses Std., November 2005 (in Japanese).

[3] W. Butler, P. Poitevin, and J. Bjomholt, "Benefits of wide area intrusion detection systems using fmcw radar," in *Security Technology, 2007 41st Annual IEEE International Carnahan Conference on*, October 2007, pp. 176–182.

[4] A. E. Cetin, O. N. Gerek, and Y. Yardimci, "Equiripple fir filter design by the fft algorithm," *IEEE Signal Processing Magazine*, vol. 14, no. 2, pp. 60–64, March 1997.

[5] E. Fishler, A. Haimovich, R. Blum, D. Chizhik, L. Cimini, and R. Valenzuela, "Mimo radar: An idea whose time has come," in *Radar Conference, 2004. Proceedings of the IEEE*, April 2004, pp. 71–78.

[6] S. Fujimori, T. Uebo, and T. Iritani, "Short-range high-resolution radar utilizing standing wave for measuring of distance and velocity of a moving target," *Electronics and Communications in Japan Part I - Communications*, vol. 89, no. 5, pp. 52–60, January 2006.

[7] ICNIRP, "ICNIRP statment on the guidelines for limiting exposure to time-varing electric, mangetic, and electromagnetic fields (up to 300 ghz)," *Health Physics*, vol. 97, no. 3, pp. 257–258, 2009.

[8] *IEEE Std C95.1-2005, IEEE Standard for Safety Levels with Respect to Human Exposure to Radio Frequency Electromagnetic Fields, 3 kHz to 300 GHz*, IEEE Std., April 2006.

[9] P. S. Jian Li, *MIMO Radar Signal Processing*. John Wiley & Sons, Inc., October 2008.

[10] "Safety guidelines for use of radio waves," http://www.tele.soumu.go.jp/resource/j/material/dwn/guide38.pdf, Ministry of Internal Affairs and Communications, June 1990 (in Japanese).

[11] S. Miyake and Y. Makino, "Application of millimeter-wave heating to materials processing,"

IEICE transactions on electronics, vol. 86, no. 12, pp. 2365–2370, December 2003.

[12] T. Saito, T. Ninomiya, O. Isaji, T. Watanabe, H. Suzuki, and N. Okubo, "Automotive fm-cw radar with heterodyne receiver," *IEICE transactions on communications*, vol. 79, no. 12, pp. 1806–1812, December 1996.

[13] W. K. Saunders, "Post-war developments in continuous-wave and frequency-modulated radar," *IRE Transactions on Aerospace and Navigational Electronics*, vol. ANE-8, no. 1, pp. 7–19, March 1961.

[14] W. Sediono and A. Lestari, "2d image reconstruction of radar indera," in *Mechatronics (ICOM), 2011 4th International Conference On*, May 2011, pp. 1–4.

[15] M. Skolnik, *Radar Handbook, Third Edition*. McGraw-Hill Education, February 2008.

[16] M. Skolnik, *Introduction to Radar Systems*. McGraw Hill, December 2002.

[17] A. G. Stove, "Linear fmcw radar techniques," *IEE Proceedings F - Radar and Signal Processing*, vol. 139, no. 5, pp. 343–350, October 1992.

[18] Ministry of Internal Affairs and Communications, "Radio law (law no. 131)," http://www.soumu.go.jp/main_sosiki/joho_tsusin/eng/Resources/laws/2003RL.pdf, May 1950.

[19] T. Uebo, Y. Okubo, and T. Iritani, "Standing wave radar capable of measuring distances sown to zero meters," *IEICE Transactions on Communications*, vol. 88, no. 6, pp. 2609–2615, June 2005.

[20] K. Yamaguchi, M. Saito, T. Akiyama, T. Kobayashi, and H. Matsue, "A 24 ghz band fm-cw radar system for detecting closed multiple targets with small displacement," in *Ubiquitous and Future Networks (ICUFN), 2015 Seventh International Conference on*, July 2015, pp. 268–273.

[21] K. Yamaguchi, M. Saito, K. Miyasaka, and H. Matsue, "Design and performance of a 24 ghz band fm-cw radar system and its application," in *Wireless and Mobile, 2014 IEEE Asia Pacific Conference on*, August 2014, pp. 226–231.

APPENDIX

In general, devices using electromagnetic waves must satisfy guidelines on human exposure to electromagnetic fields, see, for example, IEEE C95.1 in USA [8] and ICNIRP in Europe [7]. MIC have instituted guidelines in Japan [10].

The developed 24 GHz band FM-CW radar in this paper has the following properties. The power of the transmitter is 7 mW, transmitting antenna gain is 11 dBi, effective radiated power is 88 mW, radiation angle of the transmitting wave is about 50 degrees, and distance between the transmitter and the person is 2.5 m. According to the radar equation, the electric field strength E and the power density P on the human body is calculated as

$$E = \sqrt{\frac{30 \times 0.088}{2.5}} = 0.65 \ [\mathrm{V/m}] \ ,$$
$$P = \frac{E^2}{z_0} = \frac{0.65^2}{120\pi} = 1.12 \times 10^{-4} \ [\mathrm{mW/cm^2}] \ .$$

According to the guideline in [10], these parameters must satisfy

$$E \leq 61.4 \ [\mathrm{V/m}] \ ,$$
$$P \leq 1 \ [\mathrm{mW/cm^2}] \ .$$

Therefore, the developed 24 GHz band FM-CW radar system in this paper sufficiently satisfies the conditions in the guideline.

AUTHOR BIOGRAPHIES

Kazuhiro Yamaguchi was received the M.S. and Ph.D. degrees in information science from Hokkaido University, Hokkaido, Japan, in 2009 and 2012. He is currently an Assistant Professor at the Tokyo University of Science, Suwa, in Japan. His research interests include Internet of Things, wireless communication, signal and image processing, and holography.

Mitsumasa Saito was received the B.S. degree from University of Electro-communications, Tokyo, Japan, in 1978. From 1978 to 2006, he has been engaged in research and development of security and multimedia devices, electronic display for consumer electronics at SONY Corporation in Japan. In 2009, he established company of CQ-S net Inc. Kanagawa, Japan. His research interests include Internet of Things, radar technology, and signal and image processing.

Takuya Akiyama was received the B.E. and M.S. degrees from Tokyo University of Science, Suwa, Japan, in 2014 and 2016. His research interests include digital signal processing and wireless communication.

Tomohiro Kobayashi was received the B.E. degree from Tokyo University of Science, Suwa, Japan, in 2015. He is currently working toward the M.S. degree. His research interests include digital signal processing and wireless communication.

Naoki Ginoza was received the B.E. degree from Tokyo University of Science, Suwa, Japan, in 2016. He is currently working toward the M.S. degree. His research interests include digital signal processing and wireless communication.

Hideaki Matsue was received the B.S. and Ph.D. degree from University of Electro-communications and Tokyo Institute of Technology, Tokyo, Japan, in 1978 and 1993, respectively. From 1978 to 2004, he has been engaged in research and development of digital microwave radio-relay system, network architecture for personal communication at NTT Electrical Communication Laboratories in Japan. He is currently a Professor at the Tokyo University of Science, Suwa, in Japan. His research interests include Internet of Things, network architecture, and wireless communication.